Optimization of power deposition and a heating strategy for external ultrasound thermal therapy

Win-Li Lin[a)]
Institute of Biomedical Engineering, National Taiwan University, Taipei, Taiwan

Tzu-Chen Liang and Jia-Yush Yen
Department of Mechanical Engineering, National Taiwan University, Taipei, Taiwan

Hao-Li Liu and Yung-Yaw Chen
Department of Electrical Engineering, National Taiwan University, Taipei, Taiwan

(Received 27 March 2001; accepted for publication 7 August 2001)

The purpose of this paper is to examine the thermal dose distribution, to configure the optimal absorbed power deposition, and to design an appropriate heating strategy for ultrasound thermal therapy. This work employs simulation programs, which are based on the transient bio-heat transfer equation and an ideal absorbed power deposition or an ideal temperature elevation within a cube of tissue, to study the optimal absorbed power deposition. Meanwhile, a simplified model of a scanned ultrasound transducer power deposition (a cone with convergent/divergent shape) is used to investigate the heating strategy for a large tumor with a sequence of heating pulses. The distribution of thermal dose equivalence defined by Sapareto and Dewey [Int. J. Radiat. Oncol., Biol., Phys. **10**, 787–800 (1984)] is used to evaluate the heating result for a set of given parameters. The parameters considered are the absorbed power density, heating duration, temperature elevation, blood perfusion, and the size of heating cube. The results demonstrate that the peak temperature is the key factor determining the thermal dose for this short-duration heating. Heat conduction has a very strong influence on the responses of temperature and thermal dose for a small heating cube and the boundary portion of a large heating cube. Hence, for obtaining the same therapeutic result, a higher power density is required for these two conditions to compensate the great temperature difference between the heating cube and the surrounding tissue. The influence of blood perfusion on the thermal dose is negligible on the boundary portion of the heating cube, while in the central portion it may become a crucial factor as a lower power density is used in this portion to save the delivered energy. When using external ultrasound heating method to treat a large tumor, the size of heating unit, the sequence of heating pulses, and the cooling-time interval between the consecutive heating pulses are the important factors to be determined to have an appropriate treatment within a reasonable overall treatment time.
[DOI: 10.1118/1.1406516]

Key words: ultrasound thermal therapy, peak temperature, conduction, heating strategy

I. INTRODUCTION

High-intensity short-duration focused ultrasound[2–4] can be used to deliver the acoustic energy in a predetermined region to above an intensity/temperature threshold value[5–8] sufficient for necrosis. When the treatment volume is large a sequence of lesions is necessary by using this ultrasound surgery[9–15] to cover the entire treatment region and an unwanted prefocal heating may appear.[2,16–18] To reduce this problem, some cooling time is required between the lesions and consequently the total treatment time increases.[18,19] Wan *et al.*[17] investigated the possibility of using a spherical-section phased array to generate multiple-focus patterns to reduce the overall treatment time. Their results showed that the strategy with nonscanned simultaneous multiple-focus required the smallest maximum intensity and dose, resulted in the most uniform dose distribution, and significantly reduced the treatment time. Furthermore, Daum and Hynynen[20] used a 16-element, spherically sectioned array to optimize thermal dose in ultrasound surgery using the mode scanning technique with power level determined numerically. By optimizing the thermal dose over a tissue volume, the peak temperature is decreased, less average power is expended, and the overall treatment time is shortened. The absorbed power deposition, heating duration, peak temperature, size of heating cube of tissue, blood perfusion in the tissues, and the heating sequence are the parameters that potentially affect the temperature distribution and the thermal dose during ultrasound thermal therapy.

This work examines the relationship between the above parameters and the thermal dose distribution by employing an ideal absorbed power deposition and an ideal temperature elevation for a heating cube of tissue. Theoretical study of the sequential heating for a large tumor is based on a simplified power deposition model as a cone of convergent/divergent shape to investigate the heating unit, the cooling-time interval between the consecutive pulses, and the overheating/overdosing problem in the intervening tissue.

The results can serve as the basis for planning optimal strategy to adjust transducer output power to produce the thermal dose in the desired treatment region above the threshold, while minimizing the overall treatment time, the output power from the transducer, and the overdosing region of the normal tissue.

II. METHODS AND MATERIALS

A. Power depositions for parametric study and external ultrasound heating

Figure 1(a) shows that a desired treatment region is divided into nine units (with $1\cdot1\cdot3$ cm^3 for each one) and an ultrasound applicator is sequentially moved to treat this region using the high-intensity short-duration heating approach. The ultrasound applicator can be a two-dimensional phased array,[17,18,20] which has the ability to produce different heating patterns by changing the amplitude and phase of each array element. In addition, there is a feasibility to form an appropriate power deposition to meet the desired by varying the scan parameters of an ultrasound heating system with multiple-focused transducers.[21] The power deposition within a small heating cube is considered first to examine the relationship between temperature, thermal dose, and power deposition. For this parametric study, the power deposition within this small heating cube is further simplified as an ideal power deposition, which is the goal we try to deliver in a cube of tissue located in the central portion of the simulated tissue as shown in Fig. 1(b). The size of the heating cube of tissue is L cm, and the power is assumed directly deposited in this cube and a uniform absorption is also assumed.

When using external ultrasound method to heat a small cube of tissue, the deposition of ultrasound energy is modeled as a square cone of convergent/divergent shape as shown in Fig. 1(c). The left side with an area of $A(0)$ is regarded as the acoustic window at the skin surface for the ultrasonic beam, and the narrowest region with an area of $A(z_t)$ is regarded as the focal area at the focal depth, z_t, and the ultrasonic beam is propagated divergently beyond this zone. The total ultrasound energy is attenuated according to the exponential law and the deposition of ultrasonic intensity within the conical region is assumed as a uniform distribution at each depth.[22,23] Assuming that the ultrasound intensities are not large enough to cause wave distortion[24,25] and/or transient cavitation[26–28] and attenuation and absorption coefficients for the tissues are equal (all of the attenuated energy is absorbed in the heating field),[29] then the absorbed ultrasound power density in homogeneous and uniformly attenuating media is proportional to the ultrasound intensity. Hence, we can obtain the absorbed power density at depth z as

$$q(z)=2\alpha\cdot I(z)=2\mu\cdot\frac{Q(0)\cdot e^{-2\mu z}}{A(z)}$$

with

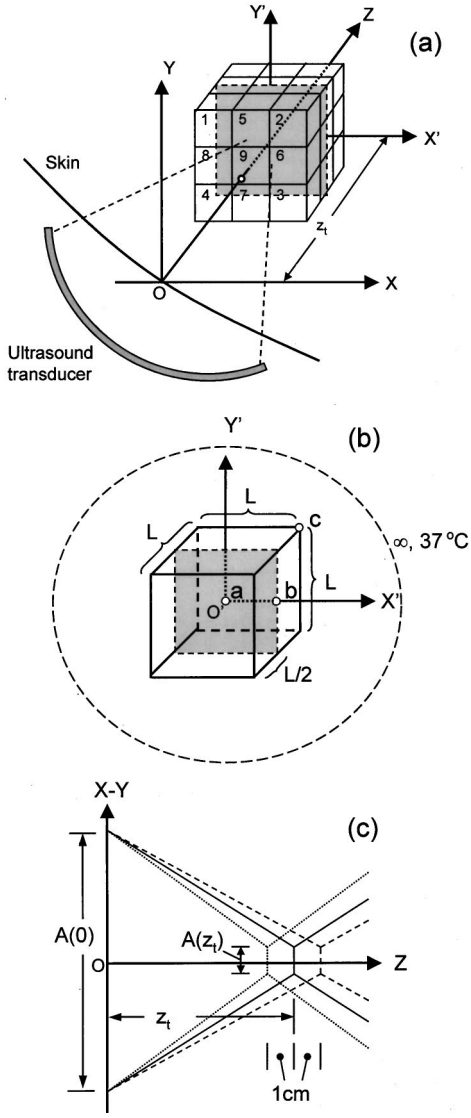

FIG. 1. Schematic diagram of the geometry studied for the distribution of thermal dose equivalence (EM_{43}) in the tissue. (a) A large, deep tumor is divided into nine heating units (with $1\cdot1\cdot3$ cm^3 for each one) and an ultrasound transducer is arranged to heat the units sequentially using the high-intensity short-duration technique; (b) a cube of tissue with a length of L cm is located in the simulated tissue, the locations of (a), (b), and (c) are (0,0,0), (0.5 L, 0, 0), and (0.5 L, 0.5 L, 0.5 L), respectively, and the responses of thermal dose on the $x'-y'$ plane and along the $o'-x'$ axis are considered in this study; (c) a triple-focal depth heating with a suitable power weighting is used for a heating unit with a dimension of $1\cdot1\cdot3$ cm^3.

$$\sqrt{A(z)}=\sqrt{A(z_t)}+(\sqrt{A(0)}-\sqrt{A(z_t)})\cdot\frac{|z-z_t|}{z_t}$$

$$(\text{from the geometry}), \tag{1}$$

where $I(z)$ and $q(z)$ are the ultrasound intensity and the absorbed power density at the depth z; α is the ultrasonic absorption coefficient of the tissue [$=\mu$: ultrasound attenuation per unit path length (5 Np m^{-1})]; $Q(0)$ denotes the total ultrasonic power propagating through the acoustic window, $A(0)$; $A(z_t)$ is the cross-sectional area with ultrasound power deposition at the focal depth z_t.

The ratio of absorbed power density at the depth z to the acoustic window is

$$SR(z;0)=\frac{q(z)}{q(0)}=\frac{2\mu\cdot\dfrac{Q(0)\cdot e^{-2\mu z}}{A(z)}}{2\mu\cdot\dfrac{Q(0)}{A(0)}}=\frac{A(0)}{A(z)}\cdot e^{-2\mu z}, \quad (2)$$

where $q(0)$ is the absorbed ultrasound power density at the acoustic window.

B. Temperature solver and thermal dose calculation

Pennes[30] transient bio-heat transfer equation (BHTE) was used to solve the temperature distribution for a given absorbed power deposition,

$$\rho c\frac{\partial T}{\partial t}=k\nabla^2 T-Wc_b(T-T_{ar})+q. \quad (3)$$

The above BHTE is a good approximation that offers a practical approach for modeling bio-thermal processes[31–33] and performing general parameter studies, even though it is a simplification neglecting the effects of discrete blood vessels and the redistribution of thermal energy within the local vascular network. We select the thermal properties to approximate averages for soft tissues.[34–36] The thermal conductivity (k) is 0.56 ($\mathrm{W\,m^{-1}\,°C^{-1}}$), the specific heat of blood (c_b) and tissue (c) is 3770 ($\mathrm{J\,kg^{-1}\,°C^{-1}}$), the tissue density ($\rho$) is 1150 $\mathrm{kg\,m^{-3}}$, the arterial temperature (T_{ar}) is 37 °C. Typical blood perfusion rates are 1–11.5, 0.15–0.5, 0.5, 0.1, 10, and 10.5 $\mathrm{kg\,m^{-3}\,s^{-1}}$ for skin, fat, muscle, bone, brain, and liver, respectively.[37] The reported perfusions of human tumors are 0.15–16 $\mathrm{kg\,m^{-3}\,s^{-1}}$, with a median value 2.9 $\mathrm{kg\,m^{-3}\,s^{-1}}$.[38] To investigate the effect of blood perfusion on the temperature and the thermal dose, a uniform perfusion (W) is assumed for the entire region and the perfusion rate is varied from 0 to 20 $\mathrm{kg\,m^{-3}\,s^{-1}}$. For the other studies, a constant value 2.0 $\mathrm{kg\,m^{-3}\,s^{-1}}$ for the entire simulated tissue is used. The anatomic and physiological properties were assumed to remain constant throughout the entire field, and metabolism was neglected due to its small contribution to temperature changes.[32,39]

The temperature change near the cube boundary is very sharp for the study of the temperature and thermal dose within a small heating cube. To assure the convergence of the simulation, the finite element method was used with a much finer mesh around the cube boundary. The transient BHTE was numerically approximated using the Frontal Solver of the commercialized software Ansys 5.4/Matlab 5.2, which is based on Finite Element Method to obtain the three-dimensional temperature field induced by the absorbed power deposition. As solving the temperature, the element size used for the heating cube is $L/12$ and that increases with the distance for the region surrounding the cube, and the number of the node is 20 for each element. The time step is between 0.02 and 2 s, depending on the speed of temperature variation. The volume of the simulated region increases greatly when using the external heating strategy to treat a region of tissue with the convergent/divergent shape of ultrasound power deposition. It is relatively advantageous to use the finite difference method to obtain the numerical solution of the three-dimensional temperature distribution for the less computational time and smaller computer memory.[40] The spatial and temporal grid sizes used are 0.5 mm and 0.05 s, respectively. In general, the accuracy of these two numerical methods is about the same.[41]

To calculate the thermal dose equivalent in minutes at 43 °C (EM_{43}) which can describe the extent of the thermal damage or destruction of tissue,[1,42,43] the Sapareto–Dewey expression[1] was used,

$$EM_{43}(\text{in min})=\int R^{(T-43)}\,dt, \quad (4)$$

where $R=2$ for $T\geqslant 43$ °C and $R=4$ for 37 °C$<T<$43 °C, T and t represent temperature and time, respectively, and EM_{43} is thermal dose equivalence in minutes. Equation (4) is used to calculate the accumulation of thermal dose at each point over the course of treatment during the simulated heating and cool-down response. The threshold dose for total necrosis ranges from $EM_{43}=30$ to 240 min for brain and muscle tissue, respectively.[4,42] For this simulation study a conservative value ($EM_{43}=300$ min) has been taken, which is similar to the analysis of Damianou *et al.*[4] for focused ultrasound surgery and Diederich and Burdette[44] for prostate ultrasound thermal therapy.

III. RESULTS

Figures 2(a) and 2(b) are the temperature responses at locations (a) and (b) as shown in Fig. 1(b) when the absorbed power density and the heating duration in Table I are given for the heating cube of tissue with a size of 10 mm. During the heating the temperature rise at the center of the cube increases almost linearly with time, especially for the shorter duration cases. For the same amount of total absorbed energy, the resulting peak temperature is higher for a shorter heating duration with a higher absorbed power density. The peak temperature is also related to the location and it declines from the center to the boundary of the cube. Figures 2(c) and 2(d) show the responses of thermal dose equivalence (EM_{43}) corresponding to the temperatures in Figs. 2(a) and 2(b), respectively. The accumulation of EM_{43} reaches its maximum faster for a shorter duration heating and its maximum value is proportional to the peak temperature. The maximum value of EM_{43} declines from the center of the cube to the boundary as the peak temperature does. Figures 2(e) and 2(f) display the resulting domain of $EM_{43}\geqslant 300$ min on the $x'-y'$ plane and the distribution of EM_{43} along the $o'-x'$ axis, respectively. These two figures indicate that a shorter duration heating produces a higher EM_{43} and a larger plateau of $EM_{43}\geqslant 300$ min for the same amount of absorbed energy. The EM_{43} on the corner of the heating cube is difficult to reach 300 min due to the very strong heat conduction; conversely the domain of $EM_{43}\geqslant 300$ min extends outside the heating cube in the normal direction of the cube's face for the shorter duration cases. Figures 2(a)–2(f) show that the accumulation of EM_{43} for the shorter duration heating is mainly from the period of temperature decaying, while the portion of this accumulation from the heating duration in-

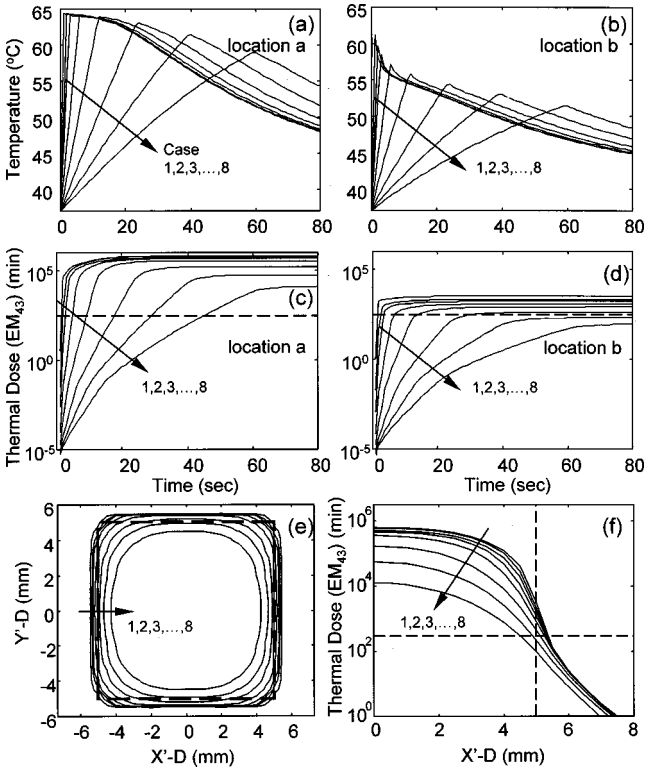

FIG. 2. (a)–(d) The responses of temperature and thermal dose at the locations (a) and (b), and (e) the contours of $EM_{43}=300$ min on the $x'-y'$ plane and (f) the thermal dose distribution along the $o'-x'$ axis for the heating cases in Table I. The horizontal dashed line in (c), (d), (f) represents $EM_{43}=300$ min and the other dashed lines in (e)–(f) are the boundary of the heating cube.

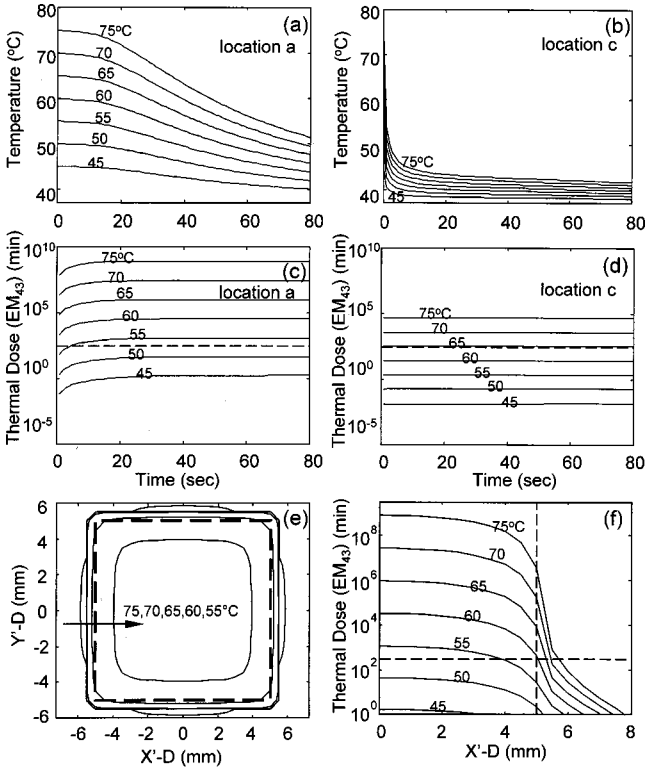

FIG. 3. (a)–(d) The responses of temperature and thermal dose at the locations (a) and (c), and (e) the contours of $EM_{43}=300$ min on the $x'-y'$ plane and (f) the thermal dose distribution along the $o'-x'$ axis when the initial temperature of the entire heating cube is set at from 45 °C to 75 °C. The horizontal dashed line in (c), (d), (f) represents $EM_{43}=300$ min, and the other dashed lines in (e)–(f) are the boundary of the heating cube.

creases for the longer duration heating and blood perfusion has more influence. For this short-duration heating, the peak temperature produced is the key factor to determine the level of EM_{43} and its distribution.

To investigate the effect of the peak temperature on the resulting thermal dose during thermal therapy, the temperature of the entire heating cube is set at from 45 °C to 75 °C as the initial condition. Figures 3(a) and 3(b), the temperature responses at locations (a) and (c), show that the effect of heat conduction on the temperature descent is highly position related. The temperature at the center of the heating cube descends very slowly, whereas on the corner it drops sharply at the very beginning. Figures 3(c) and 3(d), the responses of thermal dose corresponding to Figs. 3(a) and 3(b), display that for the same peak temperature the resulting EM_{43} at the center of the heating cube is much higher than that on the corner. The minimum peak temperature to obtain EM_{43} $\geqslant 300$ min for the center is ~ 53 °C, and this temperature is much lower than ~ 65 °C required for the corner of the heating cube. Figures 3(e) and 3(f) show the domain of EM_{43} $\geqslant 300$ min on the $x'-y'$ plane and the distribution of EM_{43} along the $o'-x'$ axis, respectively, for different peak temperatures. A higher peak temperature can produce a larger domain of $EM_{43}\geqslant 300$ min, which even covers the corner of the heating cube, while this domain shrinks to the central portion of the cube and then disappears as the peak temperature decreases.

TABLE I. The absorbed power density and the heating duration for the cube of tissue as shown in Fig. 1(b).

Case	1	2	3	4	5	6	7	8
Adsorbed power density ($W\,cm^{-3}$)	120	60	40	20	10	5	3	2
Heating duration (s)	1	2	3	6	12	24	40	60

To study the effect of blood perfusion on the temperature and the thermal dose, the peak temperature is set at 60 °C for the entire heating cube as the initial condition while the perfusion varies from 0 to 20 $kg\,m^{-3}\,s^{-1}$. Figures 4(a) and 4(b), the temperature responses for locations (a) and (b), show that the influence of perfusion on the temperature accumulates with time and the temperature differences among different perfusion levels become greater as the time passes. The temperature descent is also related to heat conduction that is a function of location. On the boundary of the heating cube, the temperature drops sharply at the very beginning due to the great temperature difference between the heating cube and the surrounding tissue. Figures 4(c) and 4(d) are the domain of $EM_{43}\geqslant 30$ min on the $x'-y'$ plane and the distributions of thermal dose along the $o'-x'$ axis, respectively. The results obviously indicate that blood perfusion affects the final level of thermal dose in the central portion of the

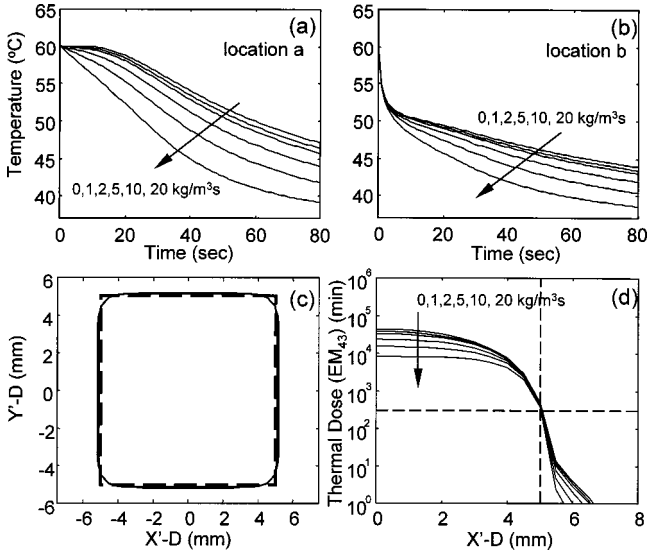

FIG. 4. (a) and (b) The temperature responses at the locations (a) and (b), as well as (c) the contours of $EM_{43}=300$ min on the $x'-y'$ plane and (d) the thermal dose distribution along the $o'-x'$ axis when the initial temperature of the entire heating cube is set at 60 °C for different blood perfusion levels. The horizontal dashed line in (d) denotes $EM_{43}=300$ min, and the other dashed lines in (c)–(d) indicate the boundary of the heating cube.

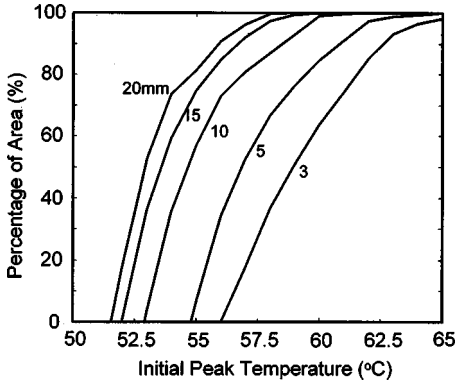

FIG. 5. Relationship among the initial peak temperature, the size of heating cube, and the percentage of area with $EM_{43}\geqslant 300$ min on the intersecting area of the heating cube and the $x'-y'$ plane.

heating cube, whereas the influence becomes trivial as approaching the boundary. On the boundary of the heating cube, the thermal doses of different blood perfusion levels converge together due to the thermal conduction is so strong that the effect of blood perfusion is almost negligible. Hence, the domain of $EM_{43}\geqslant 300$ min is actually maintained the same for different perfusion levels. This can be seen in the simulation study of Hunt *et al.*[11] and *in vivo* dog experiments[45,46] when the heating region is small the resulting thermal dose is independent of perfusion level. Conversely, the influence of blood perfusion on the thermal dose becomes greater as closer to the center of the heating cube. This indicates that blood perfusion may become an important factor when a lower power density is used in the central portion of the heating cube to save the delivered energy without knowing the magnitude of blood perfusion.

The above results show that heat conduction is the dominating factor for the responses of temperature and thermal dose on the boundary of the heating cube. Both temperature and thermal dose drop sharply on the boundary due to the heat conduction caused by the great temperature difference between the heating cube and the surrounding tissue, almost independent of blood perfusion. The thermal dose is related to the peak temperature as well as position in the heating cube, and its distribution is possibly related to the size of the heating cube due to heat conduction. To further investigate the effect of conduction on the domain of $EM_{43}\geqslant 300$ min, the size of heating cube varies from 3 to 20 mm and the peak temperature is set at from 50 °C to 65 °C as the initial condition. Figure 5 is the simulation result showing the relationship among the peak temperature, the size of the heating cube, and the percentage of the domain with $EM_{43}\geqslant 300$ min of the heating cube on the $x'-y'$ plane. The percentage of this domain increases with a larger heating cube and/or a higher peak temperature. For a smaller heating cube it requires a higher peak temperature to obtain the same percentage of $EM_{43}\geqslant 300$ min, whereas, for the same peak temperature a larger heating cube can result in a greater percentage.

The above study investigates the relationship between temperature, thermal dose, blood perfusion, and power deposition within an ideal small heating cube. When using an external heating method to treat a tumor larger than this small cube, the tumor region is divided into several units and an ultrasound transducer is moved to treat the predetermined unit sequentially. To theoretically study the sequential heating of a large tumor, the deposition of ultrasound energy for a single-focal depth heating is simply modeled as a square cone of convergent/divergent shape as shown in Fig. 1(c). This single-focal depth heating can produce a small segment, around the focal depth, with the absorbed power density (or the peak temperature) higher than the treatment requirement. For a multiple-focal depth heating, the focal depth shifted forward and backward with a proper power weighting, can produce a larger heating segment in the depth direction. By appropriately shifting the ultrasound applicator in the $x-y$ plane, a domain with $EM_{43}\geqslant 300$ min conformal to the desired treatment region can be produced. For example, the desired treatment region is a $3\cdot3\cdot3$ cm^3 cube and this treatment region is divided into nine units with a size of $1\cdot1\cdot3$ cm^3 for each one. A triple-focal depth heating is used to form a $1\cdot1\cdot3$ cm^3 with $EM_{43}\geqslant 300$ min in the depth direction as shown in Fig. 1(c) and the entire treatment region ($3\cdot3\cdot3$ cm^3) can be sequentially heated by shifting the ultrasound applicator in the $x-y$ plane as shown in Fig. 1(a).

Figure 6(a) shows the distributions of the absorbed power density ratio along the z axis and the resulting temperature just after a 6 s duration of pulse for a triple-focal depth heating. The three focal depths are located at 6, 7, and 8 cm, while the sizes of the acoustic window and the focal zone are maintained at 100 and 1 cm^2, respectively. The absorbed power density ratio for this triple-focal depth heating is calculated and scaled by using Eq. (2) for each single-focal depth heating with a power weighting of 30%, 29.5%, and 40.5% from the shallowest to the deepest. This figure dis-

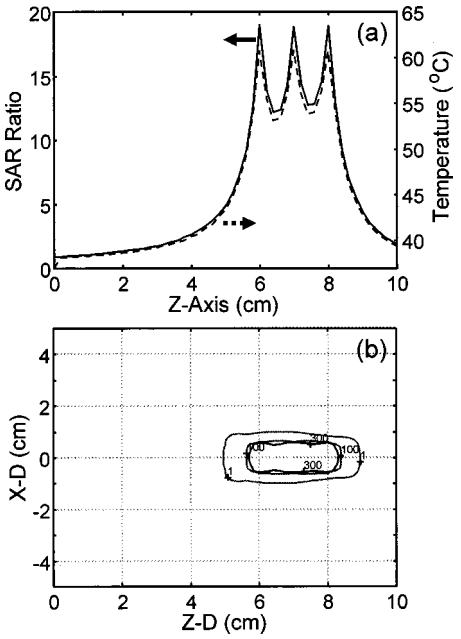

FIG. 6. The triple-focal depth heating as shown in Fig. 1(c) is used for a $1\cdot1\cdot3$ cm^3 heating unit located at 7-cm deep, while the acoustic window size is 100 cm^2 and the focal depths are located at 6, 7, and 8 cm deep with a power weighting of 30%, 29.5%, and 40.5% from the shallowest to the deepest. (a) The absorbed power density ratio (solid line) and the temperature distribution (dashed line) along the z axis, and (b) the contour of the resulting thermal dose.

plays that this approach can form a plateau of absorbed power density with three peaks within the desired treatment region and a sharp drop outside the region. These peaks in the desired treatment region indicate the three heating focal depths. The input power level is tuned to have the peak temperature at the desired treatment region to reach 60.8 °C. Figure 6(b) shows the corresponding thermal dose distribution, indicating that an appropriate thermal dose distribution for a $1\cdot1\cdot3$ cm^3 treatment unit can be achieved—the thermal dose within the unit is higher than 300 min, and it drops sharply around the boundary.

When treating a $3\cdot3\cdot3$ cm^3 cube of tissue located at 7-cm deep, the heating sequence as shown in Fig. 1(a) is used. An unwanted prefocal overheating region starting from the boundary of the predetermined treatment region may appear[2,16–18] when external ultrasound surgery with a sequence of lesions is used for a large treatment volume. To effectively reduce this problem, a temperature measurement in front of the predetermined treatment region can be used as the monitoring to determine the cooling-time interval between the consecutive heating pulses. The size of the overheated normal tissue is related to the location of the monitoring temperature and its value for starting the next heating pulse. The location should be close to the predetermined treatment region and able to sense the temperature response of each heating pulse. A lower monitoring temperature for starting the next pulse will produce a smaller overdosed region of the normal tissue, while it requires a longer overall treatment time. In this study, the temperature at (0, 0, 5) (unit: cm), 0.5 cm in front of the predetermined heating region, is employed as the monitoring to determine the cooling-time interval between the consecutive heating pulses. The heating pulse for the next unit is started when the monitoring temperature is lower than 43 °C (for the first five units) or lower than 45 °C (for the last four units). The absorbed power density at the focal locations is 17 W cm^{-3} for the first four pulses (for the four corner units), 15 W cm^{-3} for the next four pulses (for the four side units), and 13 W cm^{-3} for the last pulse (for the central unit), while the heating duration is 6 s for each pulse. Figure 7(a) shows the responses of temperature and thermal dose of the monitoring point for the entire treatment process. The first three temperature peaks are for the heating of unit 1 to 4, while the other five are for the heating from unit 5 to 9. The first temperature rise includes the first and second unit heating due to the monitoring temperature after heating the first one is lower than 43 °C. The curve of thermal dose shows that the monitoring temperature level for starting the next pulse has a strong influence on the accumulation of the thermal dose. Figures 7(b) and 7(c) display the thermal dose distributions on the $x'-y'$ plane after heating the first unit and before the heating of the fifth unit, respectively, indicating that the effective treatment region is shifted with the power deposition and the interaction influence between different heating pulses is small. Figures 7(d)–7(f) are the thermal dose distributions on the $x'-y'$, $x-z$, and $y-z$ planes, respectively, when the heating for the entire treatment region is finished and the monitoring temperature is lower than 40 °C. These figures show that the domain with $EM_{43}\geqslant 300$ min covers the entire predetermined heating cube ($3\cdot3\cdot3$ cm^3) with a small overdosed region of normal tissue in front of the predetermined region.

IV. DISCUSSION AND CONCLUSION

As a 10 mm cube of tissue is heated up to ~55 °C within a short duration the resulting thermal dose in the central portion reaches the treatment requirement ($EM_{43}\geqslant 300$ min) while it is below the requirement in the boundary region. A higher absorbed power density is required on the boundary for compensating the energy loss caused by the great temperature difference between the heating cube and the neighboring tissue, and consequentially the domain of $EM_{43}\geqslant 300$ min can be extended to cover the entire heating cube. To reduce the total amount of deposited energy a lower temperature rise can be assigned for the central portion of the heating cube and a higher temperature for the boundary portion. Figure 3(f) indicates that the deposited energy for 60 °C can be used in the boundary portion of the cube to overcome the conduction influence while the energy for 55 °C in the central portion. Therefore, the total deposited energy within this cube can be effectively reduced and this energy can be regarded as the minimum value required to produce an appropriate thermal dose distribution to cover the entire cube for this high-intensity short-duration therapy. This strategy with higher energy deposited in the boundary portion of the heating cube can be seen in Wan *et al.*[17] as well as Daum and Hynynen[20] for ultrasound thermal therapy and in Ocheltree

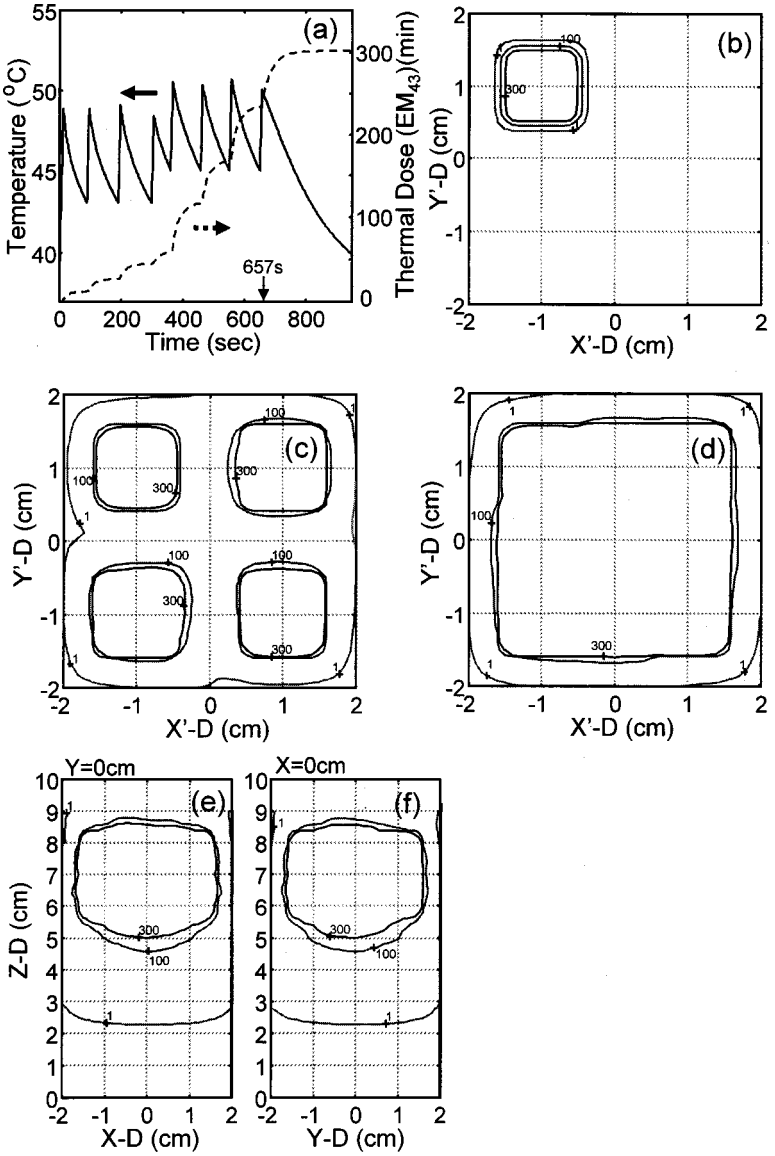

FIG. 7. The heating sequence with a heating unit of $1\cdot1\cdot3$ cm^3 as shown in Fig. 1(a) is employed for a $3\cdot3\cdot3$ cm^3 cube located at $z=7$ cm. The temperature at $z=5$ cm, 0.5 cm in front of the heating region, is used as the monitoring to determine the cooling-time intervals. (a) The responses of temperature (solid curve) and thermal dose (dashed curve) for the monitoring point during the entire treatment; (b) the thermal dose distribution on the $x'-y'$ plane before the heating of the second unit, (c) before the heating of the fifth unit, as well as (d) after the heating of all nine units and the monitoring temperature lower than 40 °C; (e)–(f) the thermal dose distribution on the $x-z$ and $y-z$ planes, respectively, for (d).

and Frizzell[47,48] for localized hyperthermia. Whereas, Fig. 2 reveals that with the same amount of total absorbed energy the temperature rise produced by a shorter duration heating is higher, indicating that the temperature required is not only related to the total absorbed energy but also to the heating duration. Accordingly, the above target temperatures (~55 °C for the central portion and 60 °C for the boundary portion of the heating cube) can be achieved by using a shorter duration heating with a smaller amount of total absorbed energy. For practical external thermal therapy, the power is delivered through an entrance window at the skin and then converged to the desired treatment region. It is important to heat the desired region effectively and efficiently in order to obtain an appropriate thermal dose distribution in the desired treatment region and also to avoid the overdosing of the normal tissue, especially in front of the desired treatment region. This denotes that with a smaller amount of total delivered energy it is better to use a shorter duration heating with a higher power density that can achieve the target temperatures for the central and the boundary portions of the heating cube, whereas the acoustic intensity used must be less than the threshold value for causing any cavitation.

In tissues with continuous wave sonication, the threshold intensity for transient cavitation has been found to be 75 W cm^{-2} at 0.368 MHz and 1450 W cm^{-2} at 2.7 MHz.[26,27] Furthermore, the results of Frizzell *et al.*[28] indicate that cavitation may be responsible for the tissue damage produced at the intensity of 289 W cm^{-2} at 1.0 MHz in vivo. Both the acoustic absorption of soft tissues[49] and the threshold intensity of transient cavitation increase with ultrasound frequency. This denotes that higher frequencies should be used in the thermal therapy for superficial tumors to avoid the cavitation problem. However, when treating deep-seated tumors, an appropriate frequency must be selected to avoid the cavitation problem and also to overcome the acoustic attenuation problem to be able to deliver enough power for the treatment. When the information of tumor size and depth is known, an appropriate frequency and a suitable size of the ultrasound transducer (related to the acoustic window size) for the treatment must be estimated based on the cavitation

threshold around the focal depth, the limitation of the transducer output power intensity, and the size of the heating unit for each pulse. Then, a proper set of the absorbed power density and the heating duration can be selected for the treatment.

When a spherical transducer is used for the high-intensity short-duration thermal therapy the lesion is relatively small with an ellipsoidal volume. The absorbed power density drops sharply from the center to the boundary of the ellipsoidal volume, and the thermal dose produced is very high at the center and then descends sharply. The absorbed power pattern is fixed and the size of the lesion is determined by the power level, heating duration, and blood perfusion. Therefore, thermal conduction and blood perfusion can affect the margin and size of the lesion as shown by Kolios *et al.*[50] during the thermal therapy unless special ultrasound beam patterns are used. Lizzi *et al.*[51] tried to use a spherical transducer with strip electrodes to generate appropriate asymmetric beams to obtain an extended lesion volume. Their *in vitro* experiment results conducted in bovine lenses show that this method is promising to reduce the number of required exposure sites and to decrease the overall treatment time needed for a large tumor volume. For a smaller heating region, the ratio of the lost energy via thermal conduction to the total absorbed energy is greater and therefore the minimum density of the deposited energy in the heating region is inversely proportional to its size for the thermal therapy. The peak temperature is almost linearly proportional to the absorbed energy density for this short-duration heating, and therefore Fig. 5 indicates the relationship between the absorbed energy density required and the size of the heating cube. For a 10 mm heating cube, the energy density for 60 °C can be used in the boundary portion of the cube, and that for 55 °C used in the central portion. However, the energy densities for 65 °C and 60 °C are required for the boundary and the central portions of the heating cube, respectively, when the cube's size reduces to 5 mm. It obviously denotes that it is more effective and efficient to have a larger cube as a heating unit during the thermal therapy. Therefore, the total energy delivered to the same volume of desired treatment region is less when the treatment region is divided into a set of larger units for a sequential heating. Consequentially, the overheating or overdosing problem in the region between the skin and the desired treatment region can be easier to avoid when a possibly larger heating unit is taken for external ultrasound thermal therapy.

The three-dimensional simulation results of Meaney *et al.*[52] and the *in vitro* experimental measurements of Malcolm and ter Haar[53] showed that the heat dissipation patterns from initial pulses in the lesion array formation could play a significant role in the heating patterns for later pulses during focused ultrasound surgery. These results indicate that an appropriate heating sequence is necessarily arranged to reduce the accumulation of the absorbed energy and the temperature rise in the intervening normal tissue between the tumor and the entrance window. Therefore, both the selection of a suitable size of heating unit and the arrangement of an appropriate heating sequence are required to avoid the overdosing of normal tissue when using external ultrasound thermal therapy to treat a large tumor. The relationship among the peak temperature, the size of heating cube, and the percentage of the domain with $EM_{43} \geqslant 300$ min for an ideal heating cube as shown in Fig. 5 indicates that the amount of the total energy required for treating the predetermined region is less when selecting a larger size of heating unit, which the heating system can achieve. This will result in having a less amount of the accumulated energy in the intervening tissue due to the overlapping of power deposition when the heating pulses shift from one unit to another during the treatment.[17,18,20] The treatable size of heating unit is related to the tumor depth/location and the entrance window of the ultrasound beam, which is determined by the heating system. The minimum size of entrance window required for ultrasound hyperthermia can be calculated based on the power attenuation and the geometrical gain,[29] as well as based on the temperature distribution.[54] A similar concept can be used to determine the treatable size of heating unit for each pulse based on the power attenuation, the geometrical gain, the limitation of the output power intensity of the transducer, and the threshold intensity of transient cavitation, when a specific acoustic window size is given.

In addition to the treatable size of heating unit, a suitable cooling-time interval between the consecutive heating pulses can be used to effectively decrease the overheating/ overdosing of the intervening normal tissue. In this study, the temperature of some point in front of the predetermined treatment region is employed as the monitoring to control the cooling-time interval. As this point's temperature is lower than some level, the next heating pulse is then started. However, this cooling interval prolongs the entire treatment process and may reduce the benefit of the high-intensity short-duration technique, especially for a large treatment volume. Some compromise is necessary between the overall treatment time and the overdosing in the normal tissue by selecting the monitoring temperature level for the next heating pulse. Furthermore, to have a more uniform thermal dose distribution within the predetermined treatment region and a shorter overall treatment time, the heating sequence can start from the four corners of the predetermined treatment region with a little more absorbed power density and then to the four sides and the center with a little less absorbed power density. The results (Fig. 7) of the proposed heating strategy denote that the use of the cooling-time interval can effectively reduce the overheating/ overdosing problem of the normal tissue within a reasonable treatment time (totally 657 s from the start of the first pulse to the end of the last) for a $3 \cdot 3 \cdot 3$ cm^3 treatment volume located at 7 cm deep. For a large tumor it may use the combination of conventional hyperthermia and thermal surgery technique—the former one for the low perfusion region and the latter for high perfusion and blood vessels.[55]

For this short-duration heating technique, the amount of absorbed energy density to obtain a given peak temperature is related to the blood perfusion level and the length of the heating duration. As the heating duration gets shorter, the amount of the energy taken away by blood perfusion during

the heating is less and the effect of blood perfusion on the resulting peak temperature is smaller. While, the influence of blood perfusion is considerable for a high blood perfusion situation with a long heating duration. This can be seen in Fig. 2(a) that the peak temperature decreases for a longer heating duration and in Figs. 4(a) and 4(d) that the temperature drops faster and the resulting thermal dose decreases for a higher blood perfusion. As shown in Fig. 2(a), the peak temperatures are about the same for the first six cases and their values are about equal to the absorbed energy density divided by the product of tissue density and specific heat. For treating a volume of tissue with high perfusion condition, it is recommended to use a shorter heating duration to reduce the effect of blood perfusion while considering the transient cavitation, the output power limitation and the treatable size of heating unit.

This study uses the absorbed power deposition and the peak temperature to investigate the responses of temperature and thermal dose in the tissue. The temperature may be higher than 60 °C for this high-intensity short-duration therapy. As the temperature approaches ~60 °C, the denaturation of the tissue occurs and the attenuation within that volume increases.[56–58] When the temperature in the tissue is higher than 60 °C during the external ultrasound thermal therapy the distribution of the power deposition may shift to form an absorbed power deposition different from the presumed pattern. The peak temperature for the predetermined treatment region is required to maintain below 60 °C, otherwise further study is necessary for the higher temperatures.

ACKNOWLEDGMENT

The authors would like to thank the National Science Council of the Republic of China for partially supporting this research under Contract No. NSC 88-2213-E-002-015.

[a]Author to whom correspondence should be addressed. Electronic mail: kcju@ipmc.ee.ntu.edu.tw

[1] S. A. Sapareto and W. C. Dewey, "Thermal dose determination in cancer therapy," Int. J. Radiat. Oncol., Biol., Phys. **10**, 787–800 (1984).
[2] C. A. Damianou and K. Hynynen, "Focal spacing and near-field heating during pulsed high temperature ultrasound therapy," Ultrasound Med. Biol. **19**, 777–787 (1993).
[3] C. A. Damianou and K. Hynynen, "The effect of various physical parameters on the size and shape of necrosed tissue volume during ultrasound surgery," J. Acoust. Soc. Am. **95**, 1641–1649 (1994).
[4] C. A. Damianou, K. Hynynen, and X. Fan, "Evaluation of accuracy of a theoretical model for predicting the necrosed tissue volume during focused ultrasound surgery," IEEE Trans. Ultrason. Ferroelectr. Freq. Control **42**, 182–187 (1995).
[5] F. Dunn and F. J. Fry, "Ultrasonic threshold dosages for the mammalaian central nervous system," IEEE Trans. Biomed. Eng. **18**, 253–256 (1971).
[6] L. A. Frizzell, C. A. Linke, and E. L. Carstenen, "Thresholds for focal ultrasonic lesions in rabbit kidney, liver and testicle," IEEE Trans. Biomed. Eng. **24**, 393–396 (1977).
[7] F. J. Fry, G. Kossof, R. C. Eggleton, and F. Dunn, "Threshold ultrasonic dosages for structural changes in mammalian brain," J. Acoust. Soc. Am. **48**, 1413–1417 (1970).
[8] T. C. Robinson and P. P. Lele, "An analysis of lesion development in the brain and in plastics by high-intensity focused ultrasound at low megahertz frequencies," J. Acoust. Soc. Am. **51**, 1333–1351 (1972).
[9] W. J. Fry, W. H. Mosberg, J. W. Barnard, and F. J. Fry, "Production of focal destructive lesions in the central nervous system with ultrasound," J. Neurosurg. **11**, 471–478 (1954).
[10] W. J. Fry, J. W. Barnard, F. J. Fry, and J. F. Brennan, "Ultrasonically produced localized selected lesions in the central nervous system," Am. J. Phys. **34**, 413–423 (1995).
[11] J. W. Hunt, R. Lalonde, H. Ginsberg, S. Urchuk, and A. Worthington, "Rapid heating: Critical theoretical assessments of thermal gradients found in hyperthermia treatments," Int. J. Hyperthermia **7**, 703–718 (1991).
[12] A. Sibille, F. Prat, J. Y. Chapelon, F. A. E. Fadil, L. Henry, Y. Theillere, T. Ponchon, and D. Cathignol, "Extracorporeal ablation of liver tissue by high-intensity focused ultrasound," Oncology **50**, 375–37 (1993).
[13] A. Sibille, F. Prat, J. Y. Chapelon, F. A. E. Fadil, L. Henry, Y. Theillere, T. Ponchon and D. Cathignol, "Characterization of extracorporeal ablation of normal and tumor-bearing liver tissue by high intensity focused ultrasound," Ultrasound Med. Biol. **19**, 803–813 (1993).
[14] G. R. ter Haar, I. Rivens, L. Chen, "High intensity focused ultrasound for the treatment of rat tumors," Phys. Med. Biol. **36**, 1495–1501 (1991).
[15] M. G. Vaughan, G. R. ter Haar, C. R. Hill, R. L. Clarke, and J. W. Hopewell, "Minimally invasive cancer surgery using focused ultrasound: A pre-clinical normal tissue study," Br. J. Radiol. **67**, 2267–274 (1994).
[16] K. Hynynen, A. Darkazanli, E. Unger, and J. F. Schenck, "MRI-guided noninvasive ultrasound surgey," Med. Phys. **20**, 107–115 (1993).
[17] H. Wan, P. VanBaren, E. S. Ebbini, and C. A. Cain, "Ultrasound surgery: Comparison of strategies using phases array systems," IEEE Trans. Ultrason. Ferroelectr. Freq. Control **43**, 1085–1098 (1996).
[18] X. Fan and K. Hynynen, "A study of various parameters of spherically curved phased arrays for noninvasive ultrasound surgery," Phys. Med. Biol. **41**, 591–608 (1996).
[19] X. Fan and K. Hynynen, "Control of the necrosed tissue volume during non-invasive ultrasound surgery using a 16-element phased array," Med. Phys. **22**, 297–306 (1995).
[20] D. R. Daum and K. Hynynen, "Thermal dose optimization via temporal switching in ultrasound surgery," IEEE Trans. Ultrason. Ferroelectr. Freq. Control **45**, 208–215 (1998).
[21] W.-L. Lin, Y.-Y. Chen, S.-Y. Lin, J.-Y. Yen, T.-S. Kuo, and M.-J. Shieh, "Optimal configuration of multiple-focused ultrasound transducers for external hyperthermia," Med. Phys. **26**, 2007–2016 (1999).
[22] E. G. Moros, R. B. Roemer, and K. Hynynen, "Pre-focal plane high temperature regions induced by scanning focused ultrasound beams," Int. J. Hyperthermia **6**, 351–366 (1990).
[23] W.-L. Lin, R. B. Roemer, E. G. Moros, and K. Hynynen, "Optimization of temperature distributions in scanned, focused ultrasound hyperthermia," Int. J. Hyperthermia **8**, 61–78 (1992).
[24] E. L. Cartensen and T. G. Muir, "The role of nonlinear acoustics in biomedical ultrasound," in *Tissue Characterization with Ultrasound*, edited by J. F. Greenleaf (CRC, Boca Raton, 1986), Vol. 1, pp. 57–79.
[25] D. Dalecki, E. L. Carstensen, K. J. Parker, and D. R. Bacon, "Absorption of finite amplitude, focused ultrasound," J. Acoust. Soc. Am. **89**, 2435–2447 (1991).
[26] P. P. Lele, "Thresholds and mechanisms of ultrasonic damage to 'organized' animal tissues," in *Symposium on Biological Effects and Characterizations of Ultrasound Sources*, edited by D. G. Hazzard and M. L. Litz (DHEW publication FDA 78-8048, United States Department of Health, Education and Welfare, Rockville, MD, 1977), pp. 224–239.
[27] F. G. Sommer and D. Pounds, "Transient cavitation in tissues during ultrasonically induced hyperthermia," Med. Phys. **9**, 1–3 (1982).
[28] L. A. Frizzell, C. S. Lee, P. D. Aschenbach, M. J. Borrelli, R. S. Morimoto, and F. Dunn, "Involvement of ultrasonically induced cavitation in the production of hind limb paralysis of the mouse neonate," J. Acoust. Soc. Am. **74**, 1062–1065 (1983).
[29] K. Hynynen, "Biophysics and technology of ultrasound hyperthermia," in *Methods of External Hyperthermic Heating*, edited by M. Gautherie (Springer, Berlin, 1990), pp. 61–116.
[30] H. H. Pennes, "Analysis of tissue and arterial blood temperatures in the resting human forearm," J. Appl. Phys. **1**, 93–122 (1948).
[31] H. Arkin, X. Xu, and K. R. Holmes, "Recent developments in modeling heat transfer in blood perfusion tissues," IEEE Trans. Biomed. Eng. **41**, 97–107 (1994).
[32] R. B. Roemer, "Thermal dosimetry," in *Thermal Dosimetry Planning*, edited by M. Gautherie (Springer, Berlin, 1990), pp. 119–214.
[33] J. C. Chato, "Fundamentals of bioheat transfer," in *Thermal Dosimetry Planning*, edited by M. Gautherie (Springer, Berlin, 1990), pp. 1–56.
[34] H. F. Bowman, "Heat transfer mechanism and thermal dosimetry," J. Natl. Cancer Inst. **61**, 437–445 (1981).

[35] J. C. Chato, ''Selected thermophysical properties of biological materials,'' in *Heat Transfer in Medicine and Biology, Analysis and Applications*, edited by A. Shitzer and R. C. Eberhart (Plenum, New York, 1985), pp. 413–418.
[36] R. G. Gordon, R. B. Roemer, and S. M. Horvath, ''A mathematical model of the human temperature regulatory system–transient cold exposure response,'' IEEE Trans. Biomed. Eng. **23**, 434–444 (1976).
[37] K. M. Sekins and A. Emery, ''Thermal science for physical medicine,'' in *Therapeutic Heat and Cold*, edited by J. Lehmann (Williams and Wilkins, Baltimore, 1982), pp. 70–132.
[38] H. Reinhold, ''Tumor microcirculation,'' in *Proceedings of 1986 NATO Advanced Study Institute on the Physics and Technology of Hyperthermia* (Nijhoff, Dordrecht, 1987), pp. 448–457.
[39] R. K. Jain, ''Bioheat transfer: Mathematical models of thermal systems,'' in *Hyperthermia Cancer Therapy*, edited by F. K. Storm (Hall, Boston, 1983), pp. 9–46.
[40] C. H. Blanchard, G. Gutierrez, J. A. White, and R. B. Roemer, ''Hybrid finite element-finite difference method for thermal analysis of blood vessels,'' Int. J. Hyperthermia **16**, 341–353 (2000).
[41] R. D. Cook, *Concepts and Applications of Finite Element Analysis* (Wiley, New York, 1981).
[42] W. C. Dewey, ''Arrhenius relationships from the molecules and cell to the clinic,'' Int. J. Hyperthermia **10**, 457–483 (1994).
[43] J. Pearce and S. Thomsen, ''Rate process analysis of thermal damage,'' in *Optical-Thermal Response of Laser-Irradiated Tissue*, edited by A. J. Welch and M. J. C. van Gemert (Plenum, New York, 1995), pp. 561–606.
[44] C. J. Diederich and E. C. Burdette, ''Transurethral ultrasound array for prostrate thermal therapy: Initial studies,'' IEEE Trans. Ultrason. Ferroelectr. Freq. Control **43**, 1011–1022 (1996).
[45] B. E. Billard, K. Hynynen, and R. B. Roemer, ''Effects of physical parameters on high temperature ultrasound hyperthermia,'' Ultrasound Med. Biol. **16**, 409–402 (1990).
[46] L. N. Dorr and K. Hynynen, ''The effect of tissue heterogeneities and large blood vessels on the thermal exposure induced by short high-power ultrasound pulses,'' Int. J. Hyperthermia **8**, 45–59 (1992).
[47] K. B. Ocheltree and L. A. Frizzell, ''Determination of power deposition patterns for localized hyperthermia: A steady state analysis,'' Int. J. Hyperthermia **3**, 269–279 (1987).
[48] K. B. Ocheltree and L. A. Frizzell, ''Determination of power deposition patterns for localized hyperthermia: A transient analysis,'' Int. J. Hyperthermia **4**, 281–296 (1988).
[49] S. A. Goss, L. A. Frizzell, and F. Dunn, ''Ultrasonic absorption and attenuation in mammalian tissues,'' Ultrasound Med. Biol. **5**, 181–186 (1979).
[50] M. C. Kolios, M. D. Sherar, and J. W. Hunt, ''Blood flow cooling and ultrasonic lesion formation,'' Med. Phys. **23**, 1287–1298 (1996).
[51] F. L. Lizzi, C. X. Deng, P. Lee, A. Rosado, R. H. Silverman, and D. J. Coleman, ''A comparison of ultrasound beams for thermal treatment of ocular tumors,'' Eur. J. Ultrasound **9**, 71–78 (1999).
[52] P. M. Meaney, R. L. Clarke, G. R. ter Haar, and I. H. Rivens, ''A 3-D finite-element model for computation of temperature profiles and regions of thermal damage during focused ultrasound surgery exposures,'' Ultrasound Med. Biol. **24**, 1489–1499 (1998).
[53] L. Malcolm and G. R. ter Haar, ''Ablation of tissue volumes using high intensity focused ultrasound,'' Ultrasound Med. Biol. **22**, 659–669 (1996).
[54] W.-L. Lin, J.-Y. Yen, Y.-Y. Chen, K.-W. Jin, and M.-J. Shieh, ''Relationship between acoustic aperture size and tumor conditions for external ultrasound hyperthermia,'' Med. Phys. **26**, 818–824 (1999).
[55] J. W. Langendijk, J. Crezee, and J. W. Hand, ''Dose uniformity in scanned focused ultrasound hyperthermia,'' Int. J. Hyperthermia **6**, 775–784 (1994).
[56] N. L. Bush, I. Rivens, G. R. ter Haar, and J. C. Bamber, ''Acoustic properties of lesions generated with an ultrasound therapy system,'' Ultrasound Med. Biol. **19**, 789–801 (1993).
[57] R. L. Clarke and G. R. ter Haar, ''Temperature rise recorded during lesion formation by high-intensity focused ultrasound,'' Ultrasound Med. Biol. **23**, 299–306 (1997).
[58] C. A. Damianou, N. T. Sanghvi, F. J. Fry, and R. Maass-Moreno, ''Dependence of ultrasonic attenuation and absorption in dog soft tissues on temperature and thermal dose,'' J. Acoust. Soc. Am. **102**, 628–634 (1997).